Electron Crystallographic Study of Photosystem II of the Cyanobacterium *Synechococcus elongatus*†

P. da Fonseca, E. P. Morris, B. Hankamer, and J. Barber*

Wolfson Laboratories, Department of Biological Sciences, Imperial College of Science, Technology and Medicine, London SW7 2AY, U.K.

Received November 16, 2001; Revised Manuscript Received January 24, 2002

ABSTRACT: The determination of the structure of PSII at high resolution is required in order to fully understand its reaction mechanisms. Two-dimensional crystals of purified highly active *Synechococcus elongatus* PSII dimers were obtained by in vitro reconstitution. Images of these crystals were recorded by electron cryo-microscopy, and their analysis revealed they belong to the two-sided plane group $p22_12_1$, with unit cell parameters $a = 121$ Å, $b = 333$ Å, and $\alpha = 90°$. From these crystals, a projection map was calculated to a resolution of approximately 16 Å. The reliability of this projection map is confirmed by its close agreement with the recently presented three-dimensional model of the same complex obtained by X-ray crystallography. Comparison of the projection map of the *Synechococcus elongatus* PSII complex with data obtained by electron crystallography of the spinach PSII core dimer reveals a similar organization of the main transmembrane subunits. However, some differences in density distribution between the cyanobacterial and higher plant PSII complexes exist, especially in the outer region of the complex between CP43 and cytochrome b_{559} and adjacent to the B-helix of the D1 protein. These differences are discussed in terms of the number and organization of some of the PSII low molecular weight subunits.

Photosystem II (PSII)[1] is a pigment−protein transmembrane complex of the photosynthetic electron transport chain. It functions as a water−plastoquinone oxidoreductase in which light energy is utilized to drive the oxidation of water and release of oxygen. This reaction, the mechanisms of which are still not fully understood, is unique in biological systems and is the origin of the Earth's oxygenic atmosphere.

PSII is a dimeric complex comprising more than 25 different protein subunits per monomer, which are encoded by *psb* genes [reviewed by (*1*, *2*)]. In each PSII monomer, two proteins, known as D1 (PsbA) and D2 (PsbD), bind all the cofactors involved in the electron-transfer chain from water to plastoquinone (*3*). Each of these proteins has five transmembrane α-helices, and together they form a heterodimer that constitutes the heart of the complex. Two chlorophyll binding proteins, CP43 (PsbC) and CP47 (PsbB), are closely associated with the PSII reaction center and function as an inner light harvesting system and as intermediates in the transfer of excitation energy from the outer light harvesting complexes to the reaction center. These proteins have six transmembrane α-helices each (1−6) with a large lumenal loop between helices 5 and 6 composed of about 150 and 200 amino acids in CP43 and CP47, respectively (*4*). In addition to these major subunits, the transmembrane domain of the PSII core complex contains a number of low molecular mass proteins frequently referred to as the small subunits, which include the α (PsbE) and β (PsbF) subunits of the redox-active cytochrome b_{559} (cyt b_{559}). Apart from the transmembrane region, the PSII complex has a lumenal extrinsic domain composed of hydrophilic proteins. These extrinsic proteins are known to optimize and maintain the stability of the water oxidation site, which is composed of a cluster of four manganese atoms located close to the lumenal surface of the transmembrane domain and are in part coordinated by amino acids of the D1 protein. Within the extrinsic domain of the oxygen evolving complex (OEC), the 33 kDa manganese stabilizing protein (PsbO) is highly conserved, while the cyanobacterial PsbU and PsbV (also known as cyt c_{550}) replace PsbP and PsbQ found in higher plants and green algae (*5*).

The information so far available for the structure of the transmembrane domain of the higher plant PSII core dimer complex has been obtained by electron cryo-crystallography. These studies involved the analysis of 2D crystals obtained either of the spinach CP47−PSII reaction center (CP47−RC) subcomplex, yielding a 3D map at a resolution of 8 Å (*6*, *7*), or of the spinach PSII core dimer, for which a 9 Å projection map was initially calculated (*8*) and subsequently a 3D map was elucidated (*9*). From the analyses of these maps, it was possible to identify densities corresponding to the transmembrane α-helices of D1, D2, CP43, CP47, and cyt b_{559}. In addition, a further 10 α-helices were identified in each monomer of the core dimer complex (*9*). The PSII low molecular weight subunits, PsbH, PsbI, PsbJ, PsbK,

† This work was supported by the Biotechnology and Biological Sciences Research Council (BBSRC). P.d.F. was supported by the PRAXIS XXI Program.

* Corresponding author. Tel: +44 20 75945266. Fax: +44 20 75945267. E-mail: j.barber@ic.ac.uk.

[1] Abbreviations: CAB, chlorophyll *a*/chlorophyll *b*; CP, chlorophyll binding protein; cyt, cytochrome; 2D, two-dimensional; 3D, three-dimensional; LHCII, PSII light harvesting complex; OEC, oxygen evolving complex; PAGE, polyacrylamide gel electrophoresis; PSII, photosystem II; SDS, sodium dodecyl sulfate.

10.1021/bi0120650 CCC: $22.00
Published on Web 03/27/2002

PsbL, PsbM, PsbN, $PsbT_C$, PsbW, and PsbX, are candidates for these unassigned helices (*10*).

In the case of the 8 Å 3D map of the CP47−RC subcomplex, it was also possible to assign density to chlorophyll molecules bound to the D1/D2 heterodimer and within the six helical bundle of CP47 (*7*). In particular, it was found that PSII did not have a 'special pair' of chlorophylls similar to that which characterizes the primary donor of other types of reaction centers. Instead P680 is composed of a tetramer of monomeric chlorophylls (*11*) which has implications for the mechanisms of primary charge separation in PSII (*12*). In the case of CP47, 14 densities were attributed to chlorophyll which was located in 2 layers, 1 toward the stromal surface and the other toward the lumenal surface of the complex (*7*).

The electron crystallography studies described above represent the most detailed information to date on the structural organization of the higher plant PSII core complex. The resolution of the data is limited, however, by the size and order of the 2D crystals analyzed. PSII core preparations from other species such as thermophilic cyanobacteria are likely to be more stable than those obtained from higher plants. Such preparations could therefore be used to improve the quality of the PSII 2D crystals and hence the ultimate resolution of the subsequent electron crystallography analysis. With this in mind, PSII core complexes have been isolated from the thermophilic cyanobacterium *Synechococcus elongatus* and used to produce 2D crystals. This cyanobacterium grows at temperatures above 55 °C, and it has been shown that PSII core complexes derived from this source are more active and stable than the PSII complexes prepared from higher plants (*13*). Indeed, they have proven to be suitable for growing 3D crystals of PSII for X-ray diffraction analysis (*14*), and as a result, a 3D structural model of PSII at 3.8 Å resolution has recently been published (*15*).

Here we present an electron crystallographic analysis of *Synechococcus elongatus* PSII core dimers. This analysis has yielded a 2D projection map at a resolution of approximately 16 Å. The density distribution in the projection map agrees very closely with the model derived from X-ray crystallography (*15*). However, comparison of the *Synechococcus elongatus* projection map with that of the PSII core dimer of spinach (*8*) indicates some differences between the cyanobacterial and higher plant systems.

MATERIALS AND METHODS

Culturing of Synechococcus elongatus. Synechococcus elongatus cells were grown as a 30 L culture in an airlift fermenter using medium D as described by Castenholz (*16*) at pH 7.5, 56 °C, through which 5% carbon dioxide in air was bubbled.

Preparation and Characterization of Purified Photosystem II. PSII core dimers were purified as described previously (*17*). The method involved the preparation of thylakoid membranes, washing of phycobiliproteins from these membranes, and solubilization and isolation of PSII by anion exchange chromatography followed by sucrose density gradients. The final PSII core dimer samples were concentrated and washed to remove sucrose and glycine betaine prior to 2D crystallization.

The purified PSII samples were analyzed by their room-temperature absorbance spectra (recorded using a Shimadzu MPS-2000 spectrophotometer) and fluorescence emission at liquid nitrogen temperature (recorded in a Perkin-Elmer LS50 luminescence spectrophotometer) upon excitation at 435 and at 600 nm for chlorophyll and phycobilins, respectively. Chlorophyll quantification was performed as described by (*18*). The activity of the purified samples was determined by measuring their oxygen evolution with a Hansatech CB1D electrode, under white light illumination (5000 $\mu E \cdot m^{-2} \cdot s^{-1}$) using 1 mM dichlorobenzoquinone (DCBQ) and 1 mM $K_3Fe(CN)_6$ as electron acceptors, at an optimized temperature of 35 °C. The protein composition of the PSII samples was analyzed by the Tricine−SDS−PAGE method described by Schägger and Jagow (*19*). After electrophoresis, the D1, D2, CP43, CP47, and PsbO proteins were identified by Western blotting using antibodies specifically raised against these proteins. PsbV was detected using the heme stain method as described in (*20*).

2D Crystallization. 2D crystals of *Synechococcus elongatus* PSII core dimers were produced by in vitro reconstitution. All crystallization trials were conducted using freshly purified PSII complexes, since it was found that the quantity and quality of the crystalline areas severely decreased when the samples used had been previously frozen. Reconstitution was performed using a lipid mixture extracted from *Synechococcus elongatus* thylakoid membranes, following the same method previously described for the preparation of thylakoid lipids from spinach (*21*). The lipids isolated from cyanobacteria were dispersed by sonication into 5 mM MES−NaOH, pH 6.5, 30% (v/v) glycerol, 5 mM $MgCl_2$, 5 mM $ZnSO_4$, and 90 mM heptyl-β-D-thioglucopyranoside. The PSII sample was added to a final chlorophyll concentration of 0.75 mg/mL. Reconstitution was achieved by detergent removal during incubation in the presence of Bio-Beads, at 20 °C, for at least 2 days.

Data Acquisition and Image Processing of 2D Crystals. During the optimization of the 2D crystallization conditions, each trial was evaluated and recorded by electron microscopy of negative-stained samples, prepared using a 2% (w/v) solution of uranyl acetate, on a Philips CM100 electron microscope. When the quantity and quality of the crystalline regions were observed to be high, samples were prepared for electron cryo-microscopy by applying them to carbon-coated grids followed by flash-freezing in liquid ethane. All electron microscope grids were glow-discharged prior to the sample application in order to increase the flatness of the crystalline areas. Electron cryo-microscopy was performed on a Philips CM200-FEG microscope, at a calibrated magnification of 48600×, under low-dose conditions. The micrographs selected for image processing were digitized using a patch densitometer (*22*) at a step-size of 5 μm followed by averaging of 3 × 3 pixel regions, so that the data were eventually sampled at 3.2 Å at the specimen level. Image processing was performed using the MRC suite of programs (*23*) together with locally developed software.

RESULTS AND DISCUSSION

2D Crystals of Synechococcus elongatus PSII. The PSII core preparations used for 2D crystallization were judged to be highly pure on the basis of their absorbance and fluorescence emission spectroscopy and protein composition analysis, as previously reported (*17*). Fractionation of the

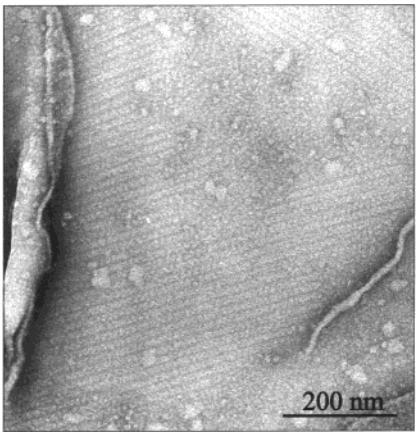

FIGURE 1: Negative-stained 2D crystals of the *Synechococcus elongatus* PSII core complex prepared by in vitro reconstitution using purified thylakoid lipids.

PSII preparation by ultracentrifugation in sucrose gradients showed that the purified complex was dimeric. These samples retained all the OEC extrinsic subunits associated with the lumenal surface and were highly active, typically evolving about 2500 μmol of O_2·(mg of chlorophyll)$^{-1}$·h^{-1}.

Crystalline sheets were formed as the result of in vitro reconstitution of *Synechococcus elongatus* PSII core dimers (Figure 1). During the optimization of the crystallization conditions, it was found that the presence of 5 mM $ZnSO_4$ during the reconstitution step was crucial for the formation of large and highly ordered 2D crystals. This effect was further enhanced by the presence of 5 mM $MgCl_2$. Although crystal patches could be clearly observed after 2 days of incubation in the presence of Bio-Beads, their quality significantly improved with time. Crystalline samples suitable for electron cryo-microscopy were harvested after at least 1 week of incubation at 20 °C in the presence of Bio-Beads. It was found that these crystals were stable for periods of at least 6 months when stored at 4 °C.

Projection Map of the Synechococcus elongatus PSII Dimer Complex. The final projection map obtained from the image processing of 2D crystals of *Synechococcus elongatus* PSII dimers is presented in Figure 2A. According to the IQ plot of the Fourier transform components used to calculate this projection map (Figure 2B), the structural data are reliable and reasonably complete to a resolution of approximately 16 Å. The crystal sheets belong to the two-sided plane group $p22_12_1$, and the unit cell parameters of these crystals are a = 121 Å, b = 333 Å, and α = 90°. One important feature of the $p22_12_1$ plane group is its set of in-plane screw axes. These screw axes arise from the PSII complexes being inserted into the reconstituted lipid membrane in two opposite orientations, so that a projection map shows both lumenal and stromal views of the complex. In projection, the stromal (yellow outline in Figure 2A) and lumenal (white outline in Figure 2A) views of the PSII complex are mirror images of each other. A significant advantage of 2D crystals with this plane group symmetry, along with other plane groups with in-plane rotation or screw axes, is that theoretically such crystal sheets can grow indefinitely and are intrinsically flat. In contrast, 2D crystals in which all molecules have the same polarity, such as the ones previously obtained for spinach PSII core complexes

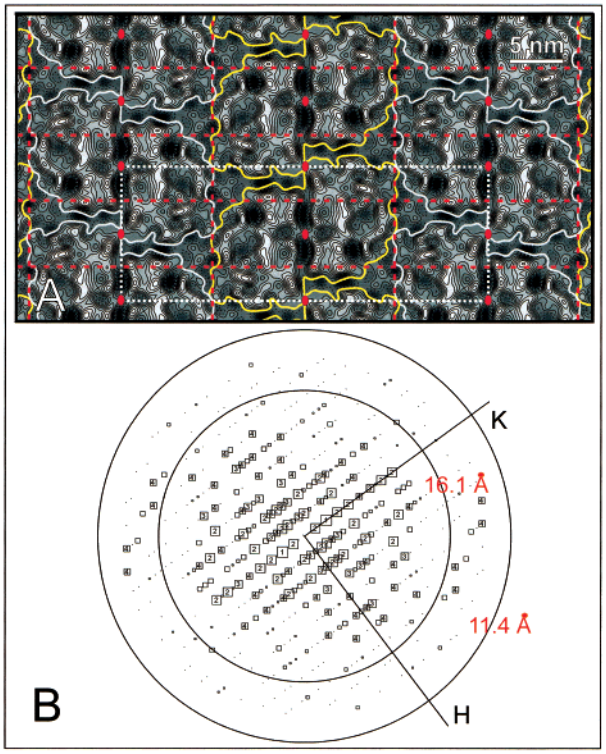

FIGURE 2: (A) Projection map determined by image processing of 2D crystals of *Synechococcus elongatus* PSII core complexes obtained after imposing full symmetry and amplitude correction, using a temperature factor of −1000. One of the unit cells is outlined in white (dotted line). These crystals belong to the two-sided plane group $p22_12_1$ (the symmetry elements are represented in red), and as a result, the projection map shows both lumenal (white outline) and stromal (yellow outline) views of the complex, which are mirror images of each other. (B) IQ plot of the Fourier components used to calculate the *Synechococcus elongatus* PSII core projection map.

(*8*, *21*), usually have a tendency to form curved sheets, which places a limit on the size and order of such crystals.

Comparison of the Structural Data on Synechococcus elongatus and Spinach PSII Core Dimer Complexes and Its Biological Relevance. The membrane spanning subunits of PSII are highly conserved between higher plants and cyanobacteria (*2*), which suggests a similar organization of their transmembrane domains. For this reason, we have compared the projection map of PSII isolated from *Synechococcus elongatus* with the 9 Å projection map obtained previously by electron crystallographic analyses of the spinach PSII core dimer complex (*8*). This comparison (shown in Figure 3) emphasizes that the PSII complexes of higher plants and cyanobacteria are dimeric. Overall they share similar density distribution, but there are some differences. In particular, the spinach projection map has a lower level of density in the region ringed in red in Figure 3. The significance of this difference can be appreciated by comparing our data with the 3D model of spinach PSII derived from electron crystallography (*9*) and that of *Synechococcus elongatus* obtained by X-ray diffraction analysis (*15*).

Figure 4A shows the 3D model of the *Synechococcus elongatus* PSII core dimer obtained by X-ray crystallography at 3.8 Å (*15*) overlaid onto our 2D projection map derived from the same complex. Although the latter is at a resolution of 16 Å, there is considerable agreement between the electron

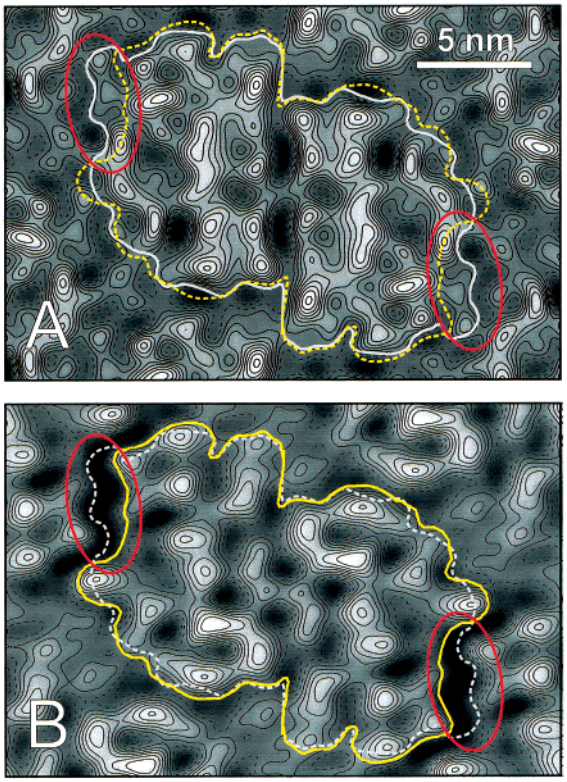

FIGURE 3: Comparison of the *Synechococcus elongatus* (A) and spinach (B) PSII core projection maps. Data in (B) were derived from (*8*). In (A), the outline of the *Synechococcus elongatus* core dimer is identified by a continuous white line, while the outline of the spinach complex is represented as a dashed yellow line. In (B), the outline of the spinach PSII core is shown as a continuos yellow line, and the *Synechococcus elongatus* PSII outline is shown as a white dashed line. The red ellipses in (A) and (B) identify the main differences between the outlines.

crystallographic data and the transmembrane domain of the 3D model derived from X-ray analysis. The projection map also clearly shows the density that corresponds to the β-strand cylindrical domain (indicated by white arrows in Figure 4A,B) assigned in the 3D model to a part of the extrinsic 33 kDa PsbO manganese stabilizing protein.

To gain a better understanding of the differences between the projection maps of *Synechococcus elongatus* and spinach, as indicated in Figure 3, we have overlaid the 3D model of the transmembrane helices of the spinach core complex obtained by electron crystallography (*9*) onto our *Synechococcus* projection map. This overlay is shown in Figure 4C, where the similarities and differences of the higher plant and cyanobacterial structures are clearly seen by comparison with the overlay of the transmembrane helices of *Synechococcus elongatus* (Figure 4B). In both models, the relative positioning of the main subunits, D1, D2, CP43, CP47, and cyt b_{559}, and their transmembrane helices is essentially identical within each monomer. Moreover, these subunits are related to each other in the same way within the dimer, emphasising the conservation of the basic structural features of PSII between higher plants and cyanobacteria. The positioning of many of the transmembrane helices of the low molecular weight subunits is also conserved between the two systems. However, the dissimilarity identified in Figure 3 relates to a lack of a cluster of transmembrane helices close to CP43 in the spinach structure compared with that of *Synechococcus*

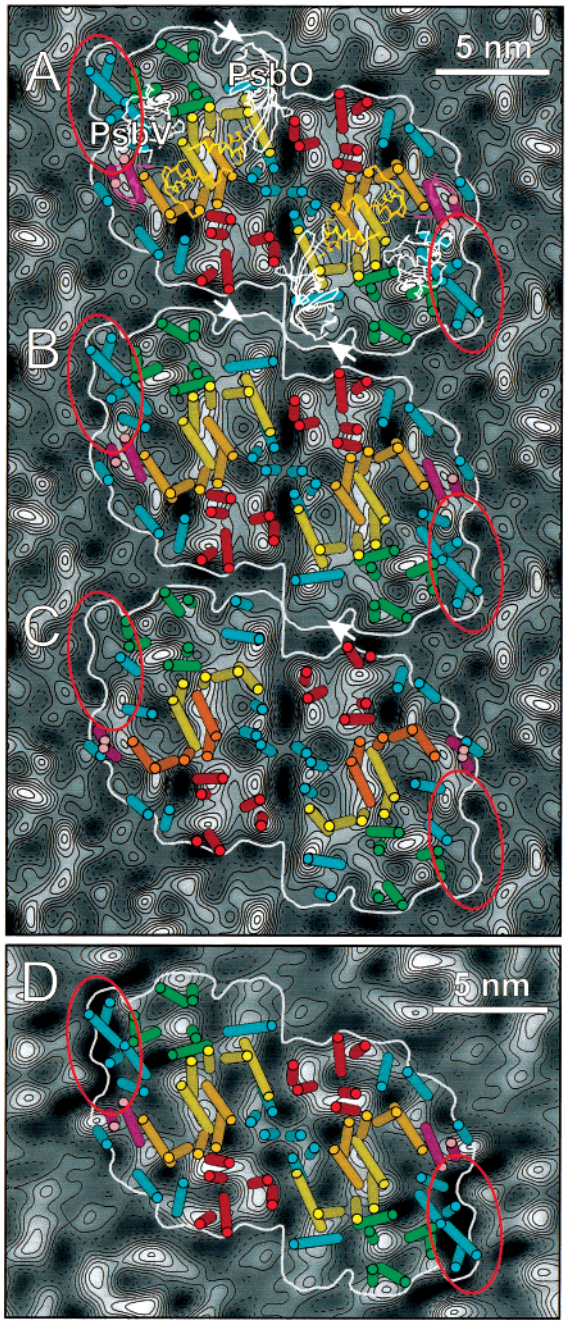

FIGURE 4: Comparison of the structural data on the PSII core dimer from *Synechococcus elongatus* and spinach. The *Synechococcus elongatus* PSII projection map, represented as contoured grayscale, is overlaid with: (A) the full 3D model of *Synechococcus elongatus* derived from X-ray crystallography (*15*); (B) the transmembrane helices of the model presented in (A); (C) the transmembrane helices of the spinach core dimer deduced from electron crystallography (*9*). (D) The 3D model of the PSII core dimer of *Synechococcus elongatus* derived from X-ray crystallography (*15*) is overlaid onto the projection map of the spinach core complex (*8*), represented as contoured grayscale. The outline of the *Synechococcus elongatus* core dimer is represented by a white line. The region corresponding to the main differences between the cyanobacterial and spinach models is indicated by red ellipses. The white arrows identify protein density assigned to a domain of the PsbO extrinsic protein. Color coding for the PSII subunits is as follows: D1 protein, yellow; D2 protein, orange; CP47, red; CP43, green; cyt b_{559}, magenta; unassigned low molecular weight subunits, blue. Extrinsic proteins (PsbO and PsbV) are in white.

elongatus (ringed in red in Figure 4). In this region, there are four helices in the *Synechococcus elongatus* PSII structure

but only one in the spinach model. However, adjacent to helix B of the D1 protein in the spinach structure, there are two transmembrane helices attributed to low molecular weight subunits but only one in the case of *Synechococcus elongatus*. These differences in the content and location of small subunits appear to reflect variations in the PSII complex between higher plants and *Synechococcus elongatus* although it is also possible that they may be related to the differential retention of particular small subunits during the preparation procedures.

The variation in the region adjacent to the CP43 subunits between the two types of PSII complex is also clearly seen by comparing the projection map of the spinach PSII core dimer complex (*8*) with the coordinates corresponding to the transmembrane domain of the *Synechococcus elongatus* PSII core complex (*15*) (Figure 4D). It is apparent both that there is insufficient space in the spinach PSII crystal lattice to accommodate the three extra transmembrane helices of the cyanobacterial system adjacent to CP43 (Figure 4D, red ellipses) and that the location of these helices corresponds to a region of minimum density in the spinach map.

Discrepancies in the small subunit composition adjacent to the CP43 subunit may be related to functional adaptations. In *Synechococcus elongatus*, this region is close to the extrinsic PsbV subunit as shown in Figure 4A. Higher plants do not have this extrinsic cytochrome and instead bind distinctly different extrinsic proteins. Also to be remembered is that cyanobacteria like *Synechococcus elongatus* have phycobiliproteins bound to the stromal surface of their PSII core complex, while the outer light-harvesting antenna of higher plants is composed of intrinsic CAB[1]proteins. It seems therefore quite reasonable to assume that given these distinct differences between higher plant and cyanobacterial systems there could be some differences within the hydrophobic regions of the PSII core dimers of the two classes of organisms. However, these differences between the plant and cyanobacterial PSII complexes are small compared to the overall structural homology of the transmembrane helices of the major subunits and many of the low molecular weight proteins.

In conclusion, the work presented here is consistent with the recently reported X-ray-derived model of the structure of PSII from *Synechococcus elongatus* (*15*). The comparison of the structural data of the *Synechococcus elongatus* PSII complex with the 3D map of the spinach PSII core dimer obtained by electron crystallography (*9*) reveals a similar organization of the major transmembrane subunits. However, differences were found between these two organisms regarding the organization of the PSII low molecular weight subunits. These differences may reflect variations between cyanobacteria and higher plants related to their different light harvesting systems and extrinsic OEC proteins. Also to be noted is that *Synechococcus elongatus* is a thermophile while spinach is not, a factor that may cause environmental adaptations and therefore may also contribute to the differences observed.

REFERENCES

1. Hankamer, B., Barber, J., and Boekema, E. (1997) *Annu. Rev. Plant Physiol. Plant Mol. Biol. 48*, 641−671.
2. Barber, J., Nield, J., Morris, E. P., Zheleva, D., and Hankamer, B. (1997) *Physiol. Plant. 100*, 817−827.
3. Diner, B. A., and Babcock, G. T. (1996) in *Oxygenic Photosynthesis: The Light Reactions* (Ort, D. R., and Yocum, C. F., Eds.) pp 137−164, Kluwer, Dordrecht, The Netherlands.
4. Bricker, T. M. (1990) *Photosynth. Res. 24*, 1−13.
5. Shen, J. R., and Inoue, Y. (1993) *Biochemistry 32*, 1825−1832.
6. Rhee, K. H. (1998) Ph.D. Thesis, University of Heidelberg, Germany.
7. Rhee, K. H., Morris, E. P., Barber, J., and Kühlbrandt, W. (1998) *Nature 396*, 283−286.
8. Hankamer, B., Morris, E. P., and Barber, J. (1999) *Nat. Struct. Biol. 6*, 560−564.
9. Hankamer, B., Morris, E. P., Gerle, C., Nield, J., and Barber, J. (2001) *J. Struct. Biol. 135*, 262−269.
10. Zheleva, D., Sharma, J., Panico, M., Morris, H. R., and Barber, J. (1998) *J. Biol. Chem. 273*, 16122−16127.
11. Barber, J., and Kühlbrandt, W. (1999) *Curr. Opin. Struct. Biol. 9*, 469−475.
12. Barber, J., and Archer, M. D. (2001) *Photobiol. Photobiochem. 142*, 97−106.
13. Schatz, G. H., and Witt, H. T. (1984) *Photobiochem. Photobiophys 7*, 1−14.
14. Zouni, A., Jordan, R., Schlodder, E., Fromme, P., and Witt, H. T. (2000) *Biochim. Biophys. Acta 1457*, 103−105.
15. Zouni, A., Witt, H. T., Kern, J., Fromme, P., Krauss, N., Saenger, W., Jordan, R., and Orth, P. (2001) *Nature 409*, 739−743.
16. Castenholz, R. W. (1969) *Bacteriol. Rev. 33*, 416−504.
17. Nield, J., Kruse, O., Ruprecht, J., da Fonseca, P., Büchel, C., and Barber, J. (2000) *J. Biol. Chem. 36*, 27940−27946.
18. Arnon, D. I. (1949) *Plant Physiol. 24*, 1−13.
19. Schägger, H., and Jagow, G. (1987) *Anal. Biochem. 166*, 368−379.
20. Thomas, P. E., Ryan, D., and Levin, W. (1976) *Anal. Biochem 75*, 168−176.
21. Morris, E. P., Hankamer, B., Zheleva, D., Friso, G., and Barber, J. (1997) *Structure 5*, 837−849.
22. Schatz, M., Zeitler, E., and van Heel, M. (1994) A high-resolution Patch Work Densitometer, International Conference on Electron Microscopy−13, pp 425−426.
23. Crowther, R. A., Henderson, R., and Smith, J. M. (1996) *J. Struct. Biol. 116*, 9−16.

BI0120650